TECHNICAL REPORTS

nature medicine

In vivo tracking of 'color-coded' effector, natural and induced regulatory T cells in the allograft response

Zhigang Fan[1,6], Joel A Spencer[2,3,6], Yan Lu[1], Costas M Pitsillides[2,4], Gurbakhshish Singh[1], Pilhan Kim[5], Seok H Yun[5], Vasilis Toxavidis[1], Terry B Strom[1], Charles P Lin[2] & Maria Koulmanda[1]

Here we present methods to longitudinally track islet allograft–infiltrating T cells in live mice by endoscopic confocal microscopy and to analyze circulating T cells by *in vivo* flow cytometry. We developed a new reporter mouse whose T cell subsets express distinct, 'color-coded' proteins enabling *in vivo* detection and identification of effector T cells (T_{eff} cells) and discrimination between natural and induced regulatory T cells (nT_{reg} and iT_{reg} cells). Using these tools, we observed marked differences in the T cell response in recipients receiving tolerance-inducing therapy (CD154-specific monoclonal antibody plus rapamycin) compared to untreated controls. These results establish real-time cell tracking as a powerful means to probe the dynamic cellular interplay mediating immunologic rejection or transplant tolerance.

Understanding the cellular immune response to transplanted tissue has a key role in developing strategies to improve transplant outcomes. Tissue biopsy is the standard method for accessing immune cell infiltration in the graft, but the method is both invasive and inadequate when temporal information is needed to characterize an immune reaction that progresses dynamically over time. Advances in molecular imaging techniques that combine cell labeling with the use of whole-body imaging modalities such as positron emission tomography, magnetic resonance imaging and bioluminescence imaging have led to promising approaches for tracking immune cells noninvasively *in vivo*[1–4], but these methods lack the sensitivity and spatial resolution to quantify events at the single-cell level. In addition, there is need to track multiple cell populations using labels that are not diluted by cell division.

Here we describe a real-time optical method for simultaneous tracking of multiple T cell subsets that are color-coded with distinct fluorescent reporters in a mouse model in which pancreatic islet transplants are placed beneath the renal capsule. As rejection occurs at 2 weeks in control untreated hosts, we track the T cell response for a period of 2 weeks after transplantation in both the circulatory compartment (by *in vivo* flow cytometry)[5] and within the allograft (by endoscopic confocal microscopy)[6]. *In vivo* flow cytometry allows noninvasive, continuous detection and quantification of fluorescently labeled cells in the circulation without the need to draw blood samples[5]. Endoscopic confocal microscopy enables minimally invasive imaging of internal organs with cellular definition by inserting a narrow-diameter endomicroscope through a small incision in the skin[6]. We show that repeated imaging of the islet allograft just beneath the renal capsule can be accomplished in the same mouse over the two-week period.

Islet transplantation is a promising clinical approach to restore insulin production and glucose regulation in patients with type 1 diabetes. The immune response to allogeneic islet transplants is $CD4^+$ T cell dependent[7–9], and includes both donor reactive, tissue-destructive T_{eff} cells and tissue-protective T_{reg} cells. The acquisition of transplant tolerance, a state in which the transplant is not rejected despite the cessation of immunosuppressive therapy, is associated with an alteration in the functional balance of T_{eff} and T_{reg} cells, as deduced in passive lymphocyte transfer experiments[10–12]. In addition, the pool of T_{reg} cells includes both nT_{reg} and iT_{reg} populations that arise during intrathymic T cell maturation or in the periphery when naive $CD4^+$ T cells are activated by antigen in the presence of transforming growth factor-β (TGF-β) and in the absence of interleukin-6 (IL-6) and IL-21, respectively[13,14]. The relative importance of iT_{reg} and nT_{reg} cells in the induction and maintenance of transplant tolerance is unclear because it has not been possible to readily distinguish these two T_{reg} subsets *in vivo*. Using our cell tracking technology, together with the color-coding scheme, we are now able to monitor not only T_{eff} and T_{reg} cells but also distinguish nT_{reg} from iT_{reg} cells in live mice to serially analyze the immune response to rejecting or tolerized major histocompatibility complex–mismatched islet transplants. As part of this study, we have tested the hypotheses that tolerance-inducing therapy will accelerate the rate and magnitude of conversion or accumulation of iT_{reg} cells from naive alloreactive T cells and lead to a profound increase in the number of allograft-infiltrating T_{reg} cells.

[1]Transplant Institute, Beth Israel Deaconess Medical Center, Harvard Medical School, Boston, Massachusetts, USA. [2]Advanced Microscopy Program, Center for Systems Biology and Wellman Center for Photomedicine, Massachusetts General Hospital, Harvard Medical School, Boston, Massachusetts, USA. [3]Department of Biomedical Engineering, Science and Technology Center, Tufts University, Medford, Massachusetts, USA. [4]Department of Biomedical Engineering, Boston University, Boston, Massachusetts, USA. [5]Advanced Microscopy Program, Wellman Center for Photomedicine, Department of Dermatology, Massachusetts General Hospital, Harvard Medical School, Boston, Massachusetts, USA. [6]These authors contributed equally to this work. Correspondence should be addressed to T.B.S. (tstrom@bidmc.harvard.edu) or C.P.L. (lin@helix.mgh.harvard.edu).

Received 29 May 2009; accepted 1 January 2010; published online 23 May 2010; doi:10.1038/nm.2155

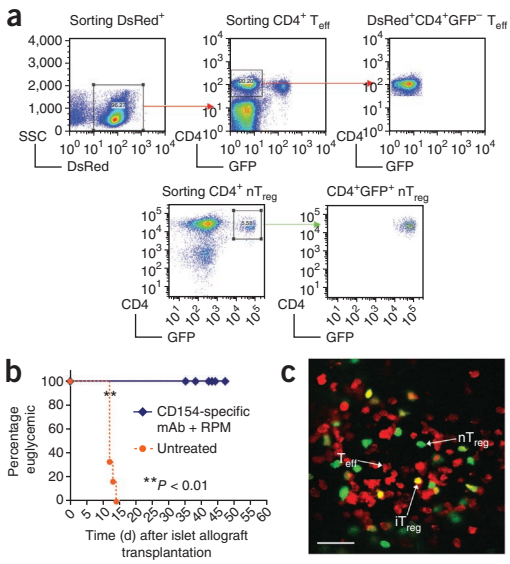

Figure 1 *In vivo* imaging of color-coded T cells. (**a**) FACS sorting of DsRed$^+$CD4$^+$GFP$^-$ red T_{eff} cells from DsRed–knock-in mice and CD4$^+$GFP$^+$ green nT_{reg} cells from the original knock-in mice. (**b**) Graft survival curves of mice treated with CD154-specific mAb plus rapamycin and untreated rejecting controls. The difference in the survival curves is significant, as calculated by either log-rank (Mantel-Cox) ($P = 0.0004$) or Gehan-Breslow-Wilcoxon ($P = 0.0012$) tests. (**c**) Representative image of allograft-infiltrating nT_{reg} (green), T_{eff} (red) and iT_{reg} cells (yellow) acquired by intravital microscopy. Scale bar, 50 μm.

RESULTS

Imaging and quantification of graft-infiltrating T cells

For islet transplantation, we first prepared C57BL/6 *Rag1*$^{-/-}$ recipient mice that lack lymphocytes by adoptive transfer of 1×10^6 nT_{reg} cells (DsRed$^-$CD4$^+$GFP$^+$) purified from C57BL/6 Foxp3-eGFP regulatory T cell reporter mice[13] together with 9×10^6 T_{eff} cells (DsRed$^+$CD4$^+$GFP$^-$) purified from C57BL/6 DsRed–knock-in mice (**Fig. 1a**). The proportion and number of transferred nT_{reg} and T_{eff} cells mimicked those present in normal wild-type mice (**Supplementary Fig. 1a**). On the next day, we placed a DBA/2 allogeneic islet graft underneath the left renal capsule (**Supplementary Fig. 1a**,**b**)[8]. One group of recipients received a tolerance-inducing protocol consisting of a 14-d course of CD154-specific monoclonal antibody (mAb) plus rapamycin. This regimen promotes conversion of antigen-activated naive T cells to iT_{reg} cells and donor-specific allograft tolerance[15]. In untreated hosts, all islet allografts were rejected by 14 d after transplantation (mean graft survival time, 12 d), whereas allografts in hosts receiving CD154-specific mAb plus rapamycin tolerizing treatment survived indefinitely (**Fig. 1b**).

We took a two-step approach to imaging the islet allograft. First, we verified our ability to identify and enumerate various T cell subsets at this location by intravital microscopy. Subsequently, we developed a minimally invasive method to accomplish these tasks through an endomicroscope.

Under appropriate conditions, CD4$^+$Foxp3$^-$ T_{eff} cells can convert into a Foxp3$^+$ phenotype, a characteristic of iT_{reg} cells[16,17]. To validate our color-coded system, we monitored *in vitro* conversion of T_{eff} to iT_{reg} cells by culturing purified T_{eff} cells collected from Ds-Red–knock-in mice (DsRed$^+$CD4$^+$GFP$^-$) with DBA/2-derived B220$^+$ splenic B cells in complete medium containing recombinant mouse TGF-β, IL-2 plus IL-4–specific and interferon-γ–specific antibodies[13,18]. Approximately 85% of T_{eff} cells cultured in these conditions acquired eGFP expression within 4 d (**Supplementary Fig. 2**), indicating their conversion to iT_{reg} cells.

Similarly, in our *in vivo* model, some DsRed$^+$CD4$^+$GFP$^-$ T_{eff} cells converted to Foxp3$^+$GFP$^+$ iT_{reg} cells after transplantation and become yellow (**Fig. 1c**). These yellow iT_{reg} cells (DsRed$^+$CD4$^+$GFP$^+$) could be readily distinguished from the green nT_{reg} cells (DsRed$^-$CD4$^+$GFP$^+$) that were originally transferred from the knock-in mice. Thus, we created a color-coded system in which T_{eff} cells were red, nT_{reg} cells were green and iT_{reg} cells were yellow (**Fig. 1c**). To verify that yellow cells were true double-positives and not an artifact created by overlapping red (T_{eff}) and green (nT_{reg}) cells within the allograft, we acquired Z-stack images in 1- to 2-μm steps (**Supplementary Video 1**) and generated reconstructed orthogonal slices (*xz* and *yz* planes) for analysis (**Supplementary Fig. 3**). Only red and green double-positive T cells that were negative in the third autofluorescence channel were identified as iT_{reg} cells (**Supplementary Fig. 4**).

Using intravital microscopy on days 1 and 4 after transplantation, very few T cells were identified within the islet allografts in either untreated hosts or hosts treated with CD154-specific mAb plus rapamycin (data not shown). On weeks 1 and 2 after transplantation, the densities of allograft-infiltrating T cells were much greater in untreated hosts than in treated hosts, with a predominant pattern of allograft infiltration by red T_{eff} cells (**Fig. 2a**). We analyzed only those images taken from the islet allograft sites, which can be readily

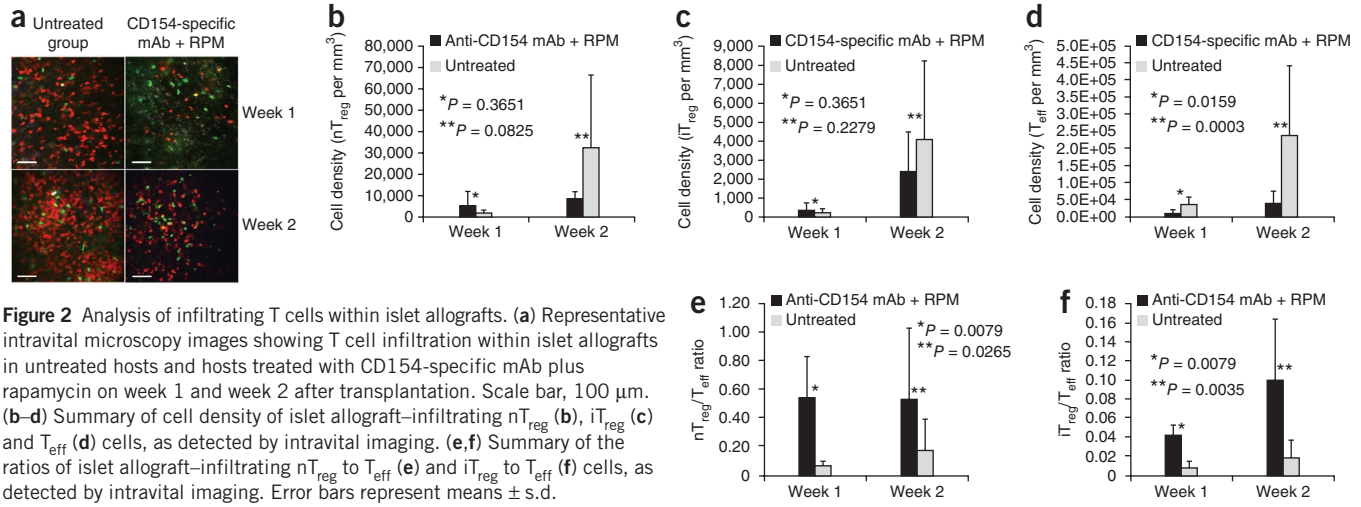

Figure 2 Analysis of infiltrating T cells within islet allografts. (**a**) Representative intravital microscopy images showing T cell infiltration within islet allografts in untreated hosts and hosts treated with CD154-specific mAb plus rapamycin on week 1 and week 2 after transplantation. Scale bar, 100 μm. (**b**–**d**) Summary of cell density of islet allograft–infiltrating nT_{reg} (**b**), iT_{reg} (**c**) and T_{eff} (**d**) cells, as detected by intravital imaging. (**e**,**f**) Summary of the ratios of islet allograft–infiltrating nT_{reg} to T_{eff} (**e**) and iT_{reg} to T_{eff} (**f**) cells, as detected by intravital imaging. Error bars represent means ± s.d.

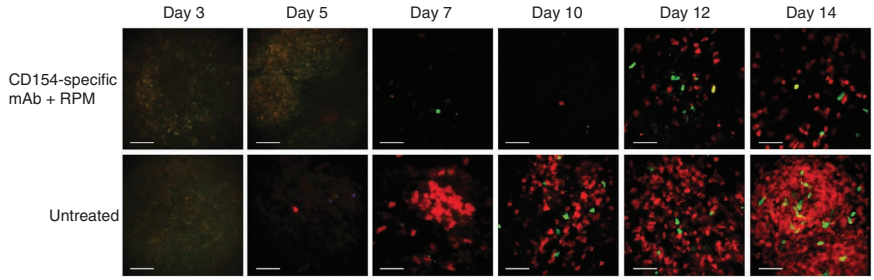

Figure 3 Serial endomicroscopy of infiltrating T cells within islet allografts. Representative endomicroscopy images within islet allografts on days 3, 5, 7, 10, 12 and 14 after transplantation in untreated hosts and hosts treated with CD154-specific mAb plus rapamycin. Each row of images is from the same mouse at the given time points. Infiltrating nT_{reg} (green), T_{eff} (red) and iT_{reg} cells (green + red) accumulate in the allograft over time. Scale bar, 50 μm.

distinguished from the surrounding kidney structure by their distinctive autofluorescence pattern (**Supplementary Fig. 5**). To our surprise, when we determined the absolute cell density of the three subsets of infiltrating T cells, the densities of allograft-infiltrating nT_{reg} and iT_{reg} cells were comparable in untreated and treated hosts at weeks 1 and 2 after transplantation (**Fig. 2b**,**c**). The prominent difference was the density of infiltrating T_{eff} cells, which was consistently and significantly higher in untreated hosts than in treated hosts at weeks 1 and 2 (**Fig. 2d**). As a result, the ratio of infiltrating nT_{reg} and iT_{reg} cells to infiltrating T_{eff} cells in treated hosts was much higher than in untreated hosts (**Fig. 2e**,**f**). Infiltration of the allograft by nT_{reg} cells was more prominent than infiltration by iT_{reg} cells.

To follow the time course of the T cell response in individual animals receiving islet transplants, we performed minimally invasive imaging with a 1.24-mm diameter endomicroscope inserted through a small incision in the skin[6]. This instrument allowed repeated imaging of the allograft site with minimal surgical manipulation and was able to resolve individual allograft infiltrating T cells (**Fig. 3**). By serially imaging the same mice at days 3, 5, 7, 10, 12 and 14 after islet transplantation, we obtained the kinetics of T cell infiltration in both the hosts treated with CD154-specific mAb plus rapamycin treated hosts and the untreated controls. Consistent with the intravital microscopy data, we observed a pronounced difference between the two hosts starting at day 7, dominated by the markedly increased number of red (T_{eff}) cells in the untreated allograft (**Fig. 3**).

Flow cytometry analysis of color-coded T cells

To test the accuracy of our color-coded system, we reconstituted C57BL/6 CD45.2$^+$ *Rag1*$^{-/-}$ mice with 1×10^6 CD45.2$^+$DsRed$^-$CD4$^+$GFP$^+$ nT_{reg} cells from knock-in mice and 9×10^6 CD45.1$^+$ DsRed$^+$CD4$^+$GFP$^-$ T_{eff} cells from CD45.1$^+$ CD45.2$^+$ (F_1 generation) DsRed–knock-in mice. Islet allografts were performed exactly as described previously[8]. We analyzed spleen samples from both untreated recipients and recipients treated with CD154-specific mAb plus rapamycin 2 weeks after transplantation (**Table 1**). In untreated hosts, 98.9% of all CD4$^+$DsRed$^+$ T cells were CD4$^+$CD45.1$^+$, whereas in treated hosts, the percentage was 96.2%. Similarly, 97.5% and 88.5% of CD4$^+$CD45.1$^+$ cells were CD4$^+$DsRed$^+$ in untreated and treated hosts, respectively. To identify false positives, we determined the percentages of CD4$^+$CD45.1$^+$ cells in the CD4$^+$DsRed$^-$ population and CD4$^+$DsRed$^+$ cells in CD4$^+$CD45.1$^-$ population. In the untreated hosts, the percentages were 2.4% and 1.1%, respectively, whereas the percentages in the treated hosts were 8.3% and 2.6%, respectively. Thus, the detection of cell subsets via analysis of cell surface CD45 isoform expression as an independent marker validated the accuracy of the color-coded system.

We used *ex vivo* flow cytometry analysis to determine the number, distribution and ratios of red T_{eff}, green nT_{reg} and yellow iT_{reg} cells in the allograft-draining lymph node at 2 weeks after islet transplantation from both untreated hosts and hosts treated with CD154-specific mAb plus rapamycin (**Supplementary Table 1**). The ratio of iT_{reg} to T_{eff} cells in the allograft was consistently elevated in treated hosts at 1 week and 2 weeks after transplantation and in the draining lymph node at 2 weeks after transplantation (**Supplementary Table 1**). The ratio of nT_{reg} to T_{eff} cells in the allograft was consistently elevated in treated hosts compared to untreated hosts at 1 week and 2 weeks after transplantation, but, in the draining lymph node at 2 weeks, the difference between treated and untreated hosts disappeared (**Supplementary Table 1**). As might be anticipated, the ratios were far more variable in spleen and nonallograft-draining peripheral lymph node, sites that are distant from the transplant (data not shown). Nonetheless, the ratios of iT_{reg} cells to T_{eff} cells and nT_{reg} cells to T_{eff} cells were consistently higher in hosts treated with CD154-specific mAb plus rapamycin compared to untreated hosts in spleen and peripheral nondraining lymph node (data not shown).

Monitoring circulating T cells by *in vivo* flow cytometry

To determine whether these T cell subtypes can be detected in the peripheral blood, we serially monitored the number of fluorescent cells flowing through an ear artery by *in vivo* flow cytometry. In both hosts treated with CD154-specific mAb plus rapamycin and untreated hosts, we detected circulating T_{eff} and nT_{reg} cells by 2 d after transplantation, and we detected iT_{reg} cells by 4 d after transplantation (**Fig. 4a**). The number of circulating T cells increased from day 2 to week 1 after transplantation, with T_{eff} cells greatly outnumbering both T_{reg} cell populations (**Fig. 4b**), but we did not identify any statistically significant difference between the two groups. Circulating T_{eff} cells were significantly more abundant in untreated hosts than in hosts treated with CD154-specific mAb plus rapamycin at week 2, at which time the allograft was undergoing rejection in the untreated control mice (**Fig. 1b**). In contrast, there was still no statistical difference in the numbers of T_{reg} cells identified in these two groups. The ratio of T_{reg} to T_{eff} cells in the circulation was significantly higher in hosts

Table 1 External validation of DsRed with the congenic marker CD45.1 by *ex vivo* flow cytometry

CD45.1$^+$ in DsRed$^+$ population	Untreated	98.9%
	CD154-specific mAb plus rapamycin	96.2%
DsRed$^+$ in CD45.1$^+$ population	Untreated	97.5%
	CD154-specific mAb plus rapamycin	88.5%
CD45.1$^+$ in DsRed$^-$ population	Untreated	2.4%
	CD154-specific mAb plus rapamycin	8.3%
DsRed$^+$ in CD45.1$^-$ population	Untreated	1.1%
	CD154-specific mAb plus rapamycin	2.6%

The correlation of the CD45.1 congenic marker with DsRed was calculated from spleen samples from the untreated mice and mice treated with CD154-specific mAb plus rapamycin on week 2 after transplantation by *ex vivo* flow cytometry on the basis of the percentage of CD4$^+$CD45.1$^+$ cells in the CD4$^+$DsRed$^+$ population and on the percentage of CD4$^+$DsRed$^+$ cells in the CD4$^+$CD45.1$^+$ population. False positives were calculated as the percentages of CD4$^+$CD45.1$^+$ cells in the CD4$^+$DsRed$^-$ population and DsRed$^+$ cells in the CD4$^+$CD45.1$^-$ population.

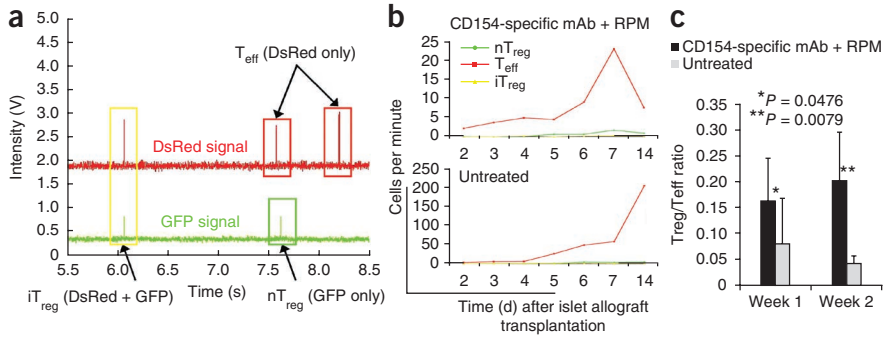

Figure 4 Detection of nT_{reg}, T_{eff} and iT_{reg} cells by *in vivo* flow cytometry in the peripheral blood. (**a**) A representative *in vivo* flow cytometry trace showing the identification of single positive nT_{reg} (green box), T_{eff} (red boxes) and double-positive iT_{reg} (yellow box) cells. The second peak in the DsRed channel occurred about 45 ms before the second peak in the GFP channel. As this time difference was greater than the uncertainty of the measurements, these two peaks were distinguished as separate cells and not a double-positive iT_{reg} cell. (**b**) *In vivo* flow cytometry showing T_{eff} (red), nT_{reg} (green) and iT_{reg} cells (yellow) in the peripheral blood. There is a ten-fold difference in scale between mice treated with CD154-specific mAb plus rapamycin and untreated mice. Each curve represents serial analysis of the same blood vessel of the same animal. (**c**) Summary of the ratio of circulating T_{reg} to T_{eff} cells, as detected by *in vivo* flow cytometry. Error bars represent means ± s.d.

treated with CD154-specific mAb plus rapamycin as compared to untreated hosts at weeks 1 and 2 after transplantation (**Fig. 4c**).

DISCUSSION

Analysis of the T cell–dependent immune response to allogeneic tissues has been hampered by the inability to serially identify iT_{reg} and nT_{reg} cell subsets in a living host. The recent development of T_{reg} cell reporter GFP knock-in mice has provided a powerful means to identify the Foxp3$^+$ T_{reg} cell population, but *Foxp3* promoter–driven GFP is expressed by both nT_{reg} and iT_{reg} cells[13,19].

We have now devised a means to serially analyze the allograft response through application of a unique tricolor-coded reporter system that enables discrimination not only between T_{eff} and T_{reg} cells but also between nT_{reg} and iT_{reg} cells. By placing islet transplants beneath the renal capsule, allograft-infiltrating T cells can be serially analyzed by endoscopic microscopy over time in the same host. Concurrently, subsets of circulating T cells can be quantified in a peripheral artery of the same living host by *in vivo* flow cytometry, without the need to draw blood samples. Compared to previous studies using traditional immunohistochemistry or standard flow cytometry that provide static 'snapshots' of T cell infiltration during allograft response[20,21], our technology allows a more complete, serial characterization of the immune response by dynamic tracking of various T cell populations both in the circulatory compartment and at the graft site of the same living host over a course of days to weeks.

With these tools, we have analyzed the T cell response to islet allografts in untreated rejecting recipients and in recipients given a transplant tolerance–inducing regimen[22,23]. The fate of the allograft, either rejection or tolerance, depends upon the functional balance of alloreactive graft–protecting T_{reg} cells to alloreactive graft–destroying T_{eff} cells[11,24–26]. In the absence of a favorable change in balance of T_{reg} to T_{eff} cells, the former cells are unable to restrain the latter cells from rejecting the transplant. Although it is known that tolerance cannot readily be induced in major histocompatibility complex–mismatched transplants in the absence of apoptosis of alloreactive T cells[22,23], the precise numeric change in the balance between T_{eff} and T_{reg} cells is not known. Moreover, it is not known whether nT_{reg} or iT_{reg} cells predominate in the graft-protective response noted in tolerized hosts. In fact, it is expected but not actually known whether these T_{reg} cell populations expand or accumulate more markedly in tolerized compared to rejecting recipients. Through the implementation of serial microendoscopy, we observed an expected increase in the of iT_{reg} to T_{eff} ratio among CD4$^+$ T cells that infiltrate the transplant in tolerized hosts as compared to rejecting hosts. Although we anticipated a massive increase in conversion or accumulation of iT_{reg} cells in tolerized as compared to rejecting hosts, this hypothesis is not supported by our data, at least within the context of our passive transfer model. We did not observe a striking numeric increase in allograft-infiltrating iT_{reg} cells in tolerized hosts compared to untreated hosts. Also unanticipated was our observation that infiltration of the allograft by nT_{reg} cells predominated over infiltration by iT_{reg} cells. The most dramatic change in the response of tolerized versus rejecting recipients was the pronounced decrease in tempo and magnitude of allograft infiltration by T_{eff} cells, a change that overshadows any change in nT_{reg} or iT_{reg} populations in tolerized hosts. As a consequence, the proportion of allograft-infiltrating T_{reg} to T_{eff} cells is very markedly enhanced in tolerized hosts. These data corroborate and give insight into the key role of reduction of the pool of donor-reactive effector T cells as a precondition for tolerance induction[22,23]. A reduction in allograft infiltration by graft destructive effector, but not regulatory, T cells enables T_{reg} cells to restrain the ability of the diminished cohort of allograft-infiltrating T_{eff} cells to reject the transplant.

In keeping with the appearance of T_{reg} cells within the allograft, we detected both nT_{reg} and iT_{reg} cells in the peripheral blood by *in vivo* flow cytometry. Indeed, we detected all three T cell subtypes in the circulation of both rejecting and tolerized hosts, days before they were discerned infiltrating the allografts. In agreement with the imaging data, we did not detect massive conversion of iT_{reg} cells in tolerized hosts, even though the technology is clearly able to detect converted iT_{reg} cells in the circulation, thereby providing unequivocal evidence of the capacity of naive T cells to convert to the Foxp3$^+$ phenotype *in vivo*. Detection of circulating iT_{reg} cells as early as day 4 after transplantation suggests that iT_{reg} conversion is an inevitable early event in the allograft response. Notably, the circulating T_{reg} to T_{eff} ratio is consistently and substantially higher in tolerized compared to rejecting hosts, raising the possibility that peripheral blood analysis can be used as an early diagnostic method, enabling more timely and effective therapy to improve transplantation outcomes.

The serial application of endoscopic confocal microscopy and *in vivo* flow cytometry to a color-coded T cell reporter system has enabled a clearer understanding of both quantitative and qualitative characteristics of the CD4$^+$ T cell response to allografts in rejecting and tolerized hosts. Indeed, the hypothesis that we held concerning the ability of co-stimulation blockade–based transplant tolerizing therapy to enable massive expansion of allograft-infiltrating T_{reg} cells, especially iT_{reg} cells, was proven incorrect. Although we have studied the allograft response in a system based on transfer of lymphocytes into lymphopenic hosts, albeit in a manner that minimizes

homeostatic proliferation, we believe application of these methods to other models will enable further progress in a meticulous dissection of the cellular and molecular basis of the allograft response. Our studies also point to a clear need for further refinement of the endoscopic imaging technique, so that serial monitoring of the cellular response in the allograft-draining lymph node with minimal invasion will become possible.

METHODS

Methods and any associated references are available in the online version of the paper at http://www.nature.com/naturemedicine/.

Note: Supplementary information is available on the Nature Medicine website.

ACKNOWLEDGMENTS

This work was supported by grants from the US National Institutes of Health (R21 AI081010 to S.H.Y. and R01 EY14106 to C.P.L. and P01-AI041521 and P01-AI041521-S1 to T.B.S.) and the Juvenile Diabetes Research Foundation (JDRF 7-2005-1329 to T.B.S. and M.K.).

AUTHOR CONTRIBUTIONS

Z.F. and J.A.S. designed the experiments, conducted research, collected and analyzed data and wrote the manuscript; Y.L., C.M.P., G.S. and V.T. helped conduct research and collected and analyzed data; P.K. and S.H.Y. developed and performed endoscopic microscopy; T.B.S., C.P.L. and M.K. designed the experiments, sponsored the project and wrote the manuscript.

COMPETING FINANCIAL INTERESTS

The authors declare no competing financial interests.

Published online at http://www.nature.com/naturemedicine/.
Reprints and permissions information is available online at http://npg.nature.com/reprintsandpermissions/.

1. Edinger, M. *et al.* Evaluation of effector cell fate and function by *in vivo* bioluminescence imaging. *Methods* **31**, 172–179 (2003).
2. Medarova, Z. *et al. In vivo* imaging of a diabetogenic $CD8^+$ T cell response during type 1 diabetes progression. *Magn. Reson. Med.* **59**, 712–720 (2008).
3. Toso, C. *et al.* Assessment of 18F-FDG-leukocyte imaging to monitor rejection after pancreatic islet transplantation. *Transplant. Proc.* **38**, 3033–3034 (2006).
4. Wu, Y.L. *et al. In situ* labeling of immune cells with iron oxide particles: an approach to detect organ rejection by cellular MRI. *Proc. Natl. Acad. Sci. USA* **103**, 1852–1857 (2006).
5. Novak, J. *et al. In vivo* flow cytometer for real-time detection and quantification of circulating cells. *Opt. Lett.* **29**, 77–79 (2004).
6. Kim, P. *et al. In vivo* confocal and multiphoton microendoscopy. *J. Biomed. Opt.* **13**, 010501 (2008).
7. Koulmanda, M. *et al.* Curative and beta cell regenerative effects of α1-antitrypsin treatment in autoimmune diabetic NOD mice. *Proc. Natl. Acad. Sci. USA* **105**, 16242–16247 (2008).
8. Koulmanda, M. *et al.* Modification of adverse inflammation is required to cure new-onset type 1 diabetic hosts. *Proc. Natl. Acad. Sci. USA* **104**, 13074–13079 (2007).
9. Tran, H.M. *et al.* Distinct mechanisms for the induction and maintenance of allograft tolerance with CTLA4-Fc treatment. *J. Immunol.* **159**, 2232–2239 (1997).
10. Sánchez-Fueyo, A. *et al.* Tim-3 inhibits T helper type 1-mediated auto- and alloimmune responses and promotes immunological tolerance. *Nat. Immunol.* **4**, 1093–1101 (2003).
11. Strom, T.B. Is transplantation tolerable? *J. Clin. Invest.* **113**, 1681–1683 (2004).
12. Strom, T.B. *et al.* The T_H1/T_H2 paradigm and the allograft response. *Curr. Opin. Immunol.* **8**, 688–693 (1996).
13. Bettelli, E. *et al.* Reciprocal developmental pathways for the generation of pathogenic effector T_H17 and regulatory T cells. *Nature* **441**, 235–238 (2006).
14. Korn, T. *et al.* IL-21 initiates an alternative pathway to induce proinflammatory T_H17 cells. *Nature* **448**, 484–487 (2007).
15. Gao, W. *et al.* Contrasting effects of cyclosporine and rapamycin in *de novo* generation of alloantigen-specific regulatory T cells. *Am. J. Transplant.* **7**, 1722–1732 (2007).
16. Fontenot, J.D., Gavin, M.A. & Rudensky, A.Y. Foxp3 programs the development and function of $CD4^+CD25^+$ regulatory T cells. *Nat. Immunol.* **4**, 330–336 (2003).
17. Wan, Y.Y. & Flavell, R.A. Identifying Foxp3-expressing suppressor T cells with a bicistronic reporter. *Proc. Natl. Acad. Sci. USA* **102**, 5126–5131 (2005).
18. Zhong, X. *et al.* Reciprocal generation of T_H1/T_H17 and T_{reg} cells by B1 and B2 B cells. *Eur. J. Immunol.* **37**, 2400–2404 (2007).
19. Fontenot, J.D. *et al.* Regulatory T cell lineage specification by the forkhead transcription factor Foxp3. *Immunity* **22**, 329–341 (2005).
20. Joffre, O. *et al.* Prevention of acute and chronic allograft rejection with $CD4^+CD25^+Foxp3^+$ regulatory T lymphocytes. *Nat. Med.* **14**, 88–92 (2008).
21. Lechler, R.I. *et al.* Organ transplantation—how much of the promise has been realized? *Nat. Med.* **11**, 605–613 (2005).
22. Li, Y. *et al.* Blocking both signal 1 and signal 2 of T cell activation prevents apoptosis of alloreactive T cells and induction of peripheral allograft tolerance. *Nat. Med.* **5**, 1298–1302 (1999).
23. Wells, A.D. *et al.* Requirement for T cell apoptosis in the induction of peripheral transplantation tolerance. *Nat. Med.* **5**, 1303–1307 (1999).
24. Kamradt, T. & Mitchison, N.A. Tolerance and autoimmunity. *N. Engl. J. Med.* **344**, 655–664 (2001).
25. Zheng, X.X. *et al.* The balance of deletion and regulation in allograft tolerance. *Immunol. Rev.* **196**, 75–84 (2003).
26. Zheng, X.X. *et al.* Favorably tipping the balance between cytopathic and regulatory T cells to create transplantation tolerance. *Immunity* **19**, 503–514 (2003).

ONLINE METHODS

Mice. DsRed–transgenic mice, in which all cells express the red fluorescent protein under the control of chicken *Actb* promoter[27] (Jackson Laboratory), and Foxp3-eGFP–knock-in mice[13], in which eGFP is specifically expressed under the control of the *Foxp3* promoter (both C57BL/6(H-2^b) background) were crossed to produce C57BL/6(H-2^b) DsRed transgenic × Foxp3-GFP–knock-in mice (DsRed–knock-in).

C57BL/6 CD45.1 transgenic mice (CD45.1^+)[28] were crossed with DsRed–knock-in (CD45.2^+) mice, and the first-generation male offspring bearing one allele of CD45.1 and one allele of CD45.2 (CD45.1^+ CD45.2^+ DsRed-Foxp3-GFP-knock-in mice) were used in the external validation experiments.

DBA/2 (H-2^d) and C57BL/6 *Rag1*$^{-/-}$ (H-2^b) mice were purchased from the Jackson Laboratory. Male mice aged 6 to 10 weeks were used as recipients and donors. Mouse use and care conformed to the guidelines established by the Animal Care Committee at Harvard Medical School and Massachusetts General Hospital.

Cell preparation and pancreatic islet transplantation. DsRed$^-$CD4$^+$GFP$^+$ nT_{reg} cells and DsRed$^+$CD4$^+$GFP$^-$ or CD45.1$^+$DsRed$^+$CD4$^+$GFP$^-$ T_{eff} cells were FACS-sorted (purity >99%) from pooled spleen and peripheral lymph nodes. In some cases, T cells were positively enriched with antibody-coated magnetic beads against CD4 (Miltenyi Biotec) before FACS sorting. CD4$^+$ T cells were analyzed for DsRed, GFP and CD45.1-APC fluorescence with FlowJo software (TreeStar).

C57BL/6 *Rag1*$^{-/-}$ mice were rendered hyperglycemic with a 275 mg per kg body weight streptozotocin[8] (Sigma-Aldrich) injection (intraperitoneally) 4 d before islet transplantation. For each C57BL/6 *Rag1*$^{-/-}$ recipient, we adoptively transferred 1×10^6 DsRed$^-$CD4$^+$GFP$^+$ nT_{reg} cells from knock-in mice and 9×10^6 DsRed$^+$CD4$^+$GFP$^-$ or CD45.1$^+$DsRed$^+$CD4$^+$GFP$^-$ T_{eff} cells from DsRed–knock-in or CD45.1-DsRed–knock-in mice 1 d before islet transplantation. Pancreatic islets were prepared by the islet core facility of Joslin Diabetes Center. Islet transplantation was performed as previously described[8]. In the group of hosts receiving tolerance-inducing therapy, 250 µg of antibody against CD154 (IgG2a, HB11048, American Type Culture Collection)[15,26] and 3 mg per kg body weight of rapamycin were injected intraperitoneally for three consecutive days starting on day 0, the day of islet transplantation. Rapamycin (3 mg per kg body weight) was then given every other day for 2 weeks. We performed serial blood glucose measurements and define allograft rejection as the first day of 3 consecutive d of blood glucose exceeding 250 mg dl^{-1}.

Intravital microscopy and image analysis. Under ketamine-xylazine anesthesia, a biocompatible hyaluronic acid gel (Healon, Advanced Medical Optics) and a No. 1 cover slip were applied directly on top of the surgically exposed kidney (**Supplementary Fig. 1b**). The mouse was mounted on a heated stage and placed under the upright objective lens of a custom- built, video-rate, laser-scanning confocal microscope[29]. GFP and DsRed were excited at 491 nm, and autofluorescence was excited at 635 nm. Images were acquired by averaging 30 video frames. Z-stacks were acquired in 2-µm steps. Immediately after imaging, the kidney was returned, the retroperitoneal cavity closed with a 5.0 Vicryl suture and the skin clipped shut using standard surgical clips.

The number of DsRed$^+$GFP$^-$ and DsRed$^-$GFP$^+$ cells was determined for each image with a custom MATLAB program and verified manually in selected cases. Three to 15 images per mouse ($n \geq 4$) per time point were quantified. The number of double-positive cells was determined for each image manually, and the resulting value was subtracted from the total DsRed$^+$GFP$^-$ and DsRed$^-$GFP$^+$ cells for that image. Cell density was the cell number divided by the sample volume, defined as the area of the image times the optical section thickness.

Endoscopic confocal microscopy and *In vivo* flow cytometry. A 1.24-mm diameter gradient index lens endomicroscope with a numerical aperture of 0.6 was used to serially image the islet allograft[6] through the small incision that was initially made for the islet transplantation on day 0. GFP, DsRed and autofluorescence signals were excited sequentially at 491, 532 and 635 nm. Images were acquired by averaging between 15 to 90 video frames. Each allograft was imaged for 15–45 min on days 3, 5, 7, 10, 12 and 14 after transplantation.

Circulating T cells were detected in an ear artery by *in vivo* flow cytometry[5]. GFP and DsRed were excited simultaneously at 473 and 561 nm. Ten to fifteen 1-min traces were recorded at each time point (days 2–7 and 14) and analyzed with a custom MATLAB program to identified single- and double-positive peaks in the two channels ($n \geq 4$ mice for both groups at each time point). The probability that a single DsRed$^+$ and a single GFP$^+$ cell accidentally overlap in a 1-min trace and is counted as a false double-positive cell is less than 0.026%.

Statistical analyses. Statistical significance was calculated with Mann-Whitney tests using SPSS software (SPSS). Kaplan-Meier survival analysis was performed with both log-rank (Mantel-Cox) and Gehan-Breslow-Wilcoxon tests (GraphPad). All *P* values of 0.05 or less were considered as significant and are referred to as such in the text. All error bars represent s.d.

27. Vintersten, K. *et al.* Mouse in red: red fluorescent protein expression in mouse ES cells, embryos and adult animals. *Genesis* **40**, 241–246 (2004).
28. Shen, F.W. *et al.* Cloning of Ly-5 cDNA. *Proc. Natl. Acad. Sci. USA* **82**, 7360–7363 (1985).
29. Veilleux, I., Spencer, J.A., Biss, D.P., Côté, D. & Lin, C.P. *In vivo* cell tracking with video rate multimodality laser scanning microscopy. *IEEE J. Sel. Top. Quantum Electron.* **14**, 10–18 (2008).